Supplement of Hydrol. Earth Syst. Sci., 26, 1295–1318, 2022
https://doi.org/10.5194/hess-26-1295-2022-supplement

Hydrology and Earth System Sciences
Open Access
EGU

Supplement of

Ecosystem adaptation to climate change: the sensitivity of hydrological predictions to time-dynamic model parameters

Laurène J. E. Bouaziz et al.

Correspondence to: Laurène J. E. Bouaziz (laurene.bouaziz@deltares.nl)

The supplement provides details on the monthly correction factors applied to the observed historical E-OBS climate data (Sect. S1). Technical details on the calculation of the root-zone storage capacities for the various scenarios are provided in Sect. S2. Model schematization, water balance equations, constitutive functions and model parameters are provided in Sects. S3 and S4. An analysis of hydrological model results obtained when the model is forced with the simulated historical climate data and the root-zone storage capacity parameter derived from this data is provided in Sect. S5.

S1 Monthly correction factors for E-OBS precipitation data

The precipitation of the observed historical E-OBS climate data is compared with the precipitation data derived from interpolated local station data for the period 2005 to 2017, as used in Bouaziz et al. (2020). There is a good level of agreement between both datasets for most of the area of the Meuse basin. However, E-OBS precipitation data underestimate the interpolated station data at the center of the basin. Differences between both datasets are likely related to the lower amount of stations used in the development of the E-OBS dataset. Correction factors are derived and applied per month for the area where the underestimation of E-OBS precipitation exceeds 20 % (Fig. S1).

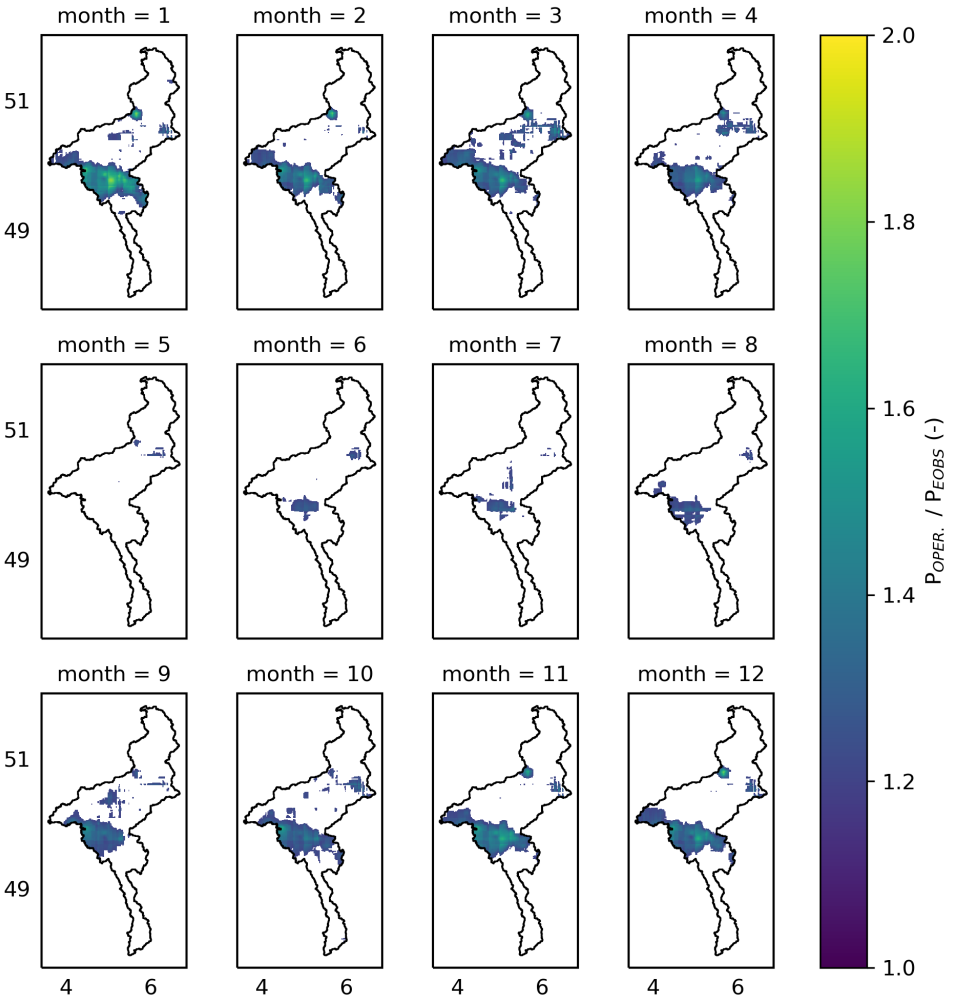

Figure S1: Monthly correction factors for the E-OBS precipitation data (P_{EOBS}) derived from the comparison with a precipitation dataset derived from interpolated local station data (denoted as $P_{\mathrm{OPER.}}$ in the legend).

S2 Technical details on the calculation of the root-zone storage capacities

Table S1 summarizes the data sources used to estimate the various root-zone storage capacities. In this study, we assume that the observed E-OBS historical climate data is the best available estimate of current-day climate conditions and use this data to estimate historical root-zone storage capacities $S_{\mathrm{R,max,A}}$ and to calibrate the hydrological model.

The simulated historical climate data is required to enable a fair comparison with the simulated 2K climate data, as they are both generated with the regional climate model. Despite potential biases in the climate model simulations compared to the observed historical data (here, E-OBS), we do not apply a formal bias-correction of the climate data which may alter the relations between variables in climate models (Ehret et al., 2012). Instead, we force the hydrological model with the native simulated historical climate data (i.e. without bias-correction) in combination with the $S_{\mathrm{R,max,A}}$ parameter. An alternative approach would have been to estimate the root-zone storage capacities using the simulated historical climate data ($S_{\mathrm{R,max,A1}}$ in Table S1), to directly correct for potential biases in the climate data in the estimation of the root-zone storage capacity parameter but with the downside of affecting spatial patterns across catchments. For comparison, this analysis is performed in Sect. S5.

Yet, to account for the bias between the observed and simulated historical climate data, we add the difference between storage deficits derived from the 2K and simulated historical climate simulations ($S_{\mathrm{R,def,2K}} - S_{\mathrm{R,def,hist}}$) to the observed storage deficits derived with E-OBS data $S_{\mathrm{R,def,obs}}$ to determine $S_{\mathrm{R,max,B}}$, $S_{\mathrm{R,max,C}}$ and $S_{\mathrm{R,max,D}}$, as shown in Table S1.

Table S1: Root-zone storage capacity description and symbols, derived from long-term transpiration and storage deficits calculations for observed historical E-OBS data (P_{obs}) and simulated historical (P_{hist}) and 2K climate data (P_{2K}) for historical land use (ω_{obs}) and land-use change scenarios ($\omega_{\mathrm{broadleaved}}$ and $\omega_{\mathrm{coniferous}}$). The overline symbol is omitted from P, Q and E_{R} to increase readability.

Description	Root-zone storage capacity $S_{\mathrm{R,max}}$ [mm]	Long-term transpiration E_{R} [mm yr^{-1}] (Eq. 5)	Storage deficit $S_{\mathrm{R,def}}$ [mm] (Eq. 7)
Observed historical climate (E-OBS) historical land use (ω_{obs})	$S_{\mathrm{R,max,A}}$	$P_{\mathrm{E,obs}} - Q_{\mathrm{obs}}$	$S_{\mathrm{R,def,obs}}$
Simulated historical climate historical land use (ω_{obs}) (historical runoff coefficient)	$S_{\mathrm{R,max,A1}}$	$P_{\mathrm{E,hist}} - Q_{\mathrm{obs}}/P_{\mathrm{obs}} \cdot P_{\mathrm{hist}}$	$S_{\mathrm{R,def,hist}}$
2K climate historical land use (ω_{obs})	$S_{\mathrm{R,max,B}}$	$P_{\mathrm{E,2K}} - (Q/P)_{\mathrm{2K,B}} \cdot P_{\mathrm{2K}}$ (Eq. 3)	$\max(\lvert S_{\mathrm{R,def,obs}} + \min(0, S_{\mathrm{R,def,2K,B}} - S_{\mathrm{R,def,hist}})\rvert)$
2K climate broadleaved land use ($\omega_{\mathrm{broadleaved}}$)	$S_{\mathrm{R,max,C}}$	$P_{\mathrm{E,2K}} - (Q/P)_{\mathrm{2K,C}} \cdot P_{\mathrm{2K}}$ (Eq. 3)	$\max(\lvert S_{\mathrm{R,def,obs}} + \min(0, S_{\mathrm{R,def,2K,C}} - S_{\mathrm{R,def,hist}})\rvert)$
2K climate coniferous land use ($\omega_{\mathrm{coniferous}}$)	$S_{\mathrm{R,max,D}}$	$P_{\mathrm{E,2K}} - (Q/P)_{\mathrm{2K,D}} \cdot P_{\mathrm{2K}}$ (Eq. 3)	$\max(\lvert S_{\mathrm{R,def,obs}} + \min(0, S_{\mathrm{R,def,2K,D}} - S_{\mathrm{R,def,hist}})\rvert)$

S3 Model schematization and equations

A schematic representation of the wflow_FLEX-Topo model with three HRUs for plateau, hillslope and wetland connected through their groundwater storage is shown in Fig. S2. The model is forced with spatially distributed precipitation, temperature and potential evaporation data. Each HRU includes storages for snow S_{W}, interception S_{I}, the root-zone S_{R}, a fast runoff component S_{F} and a common groundwater S_{S} [mm]. The total streamflow Q [mm d^{-1}] is the sum of fast runoff Q_{F} from the three HRUs and groundwater runoff Q_{S}. Evaporation [mm d^{-1}] occurs from the snow storage (E_{W}), the interception storage (E_{I}) and the root-zone storage (E_{R}). A simple formulation to express water stress is used to calculate evaporation from the root-zone storage. The equation describes how actual evaporation is linearly reduced when the root-zone storage is below a certain threshold (L_{P} parameter), as shown in Table S5.

Main differences between the three HRUs include potential differences in parameter values, the presence of percolation only in the plateau class, whereas the wetland class includes capillary rise but no preferential recharge. Parameters specific to plateau, hillslope and wetland include a maximum percolation rate $R_{\mathrm{P,max,P}}$ [mm d^{-1}], a non-linear coefficient for fast runoff α_{P} and α_{H} [-], and a maximum capillary rise rate $R_{\mathrm{C,max,W}}$ [mm d^{-1}].

Symbols used to define the different fluxes and storages in the model schematization (Fig. S2) are detailed in Table S2 and Table S3. Definitions of the symbols used for the parameters are provided in Sect. S4. Water balance and constitutive equations are provided in Table S4 and in Table S5.

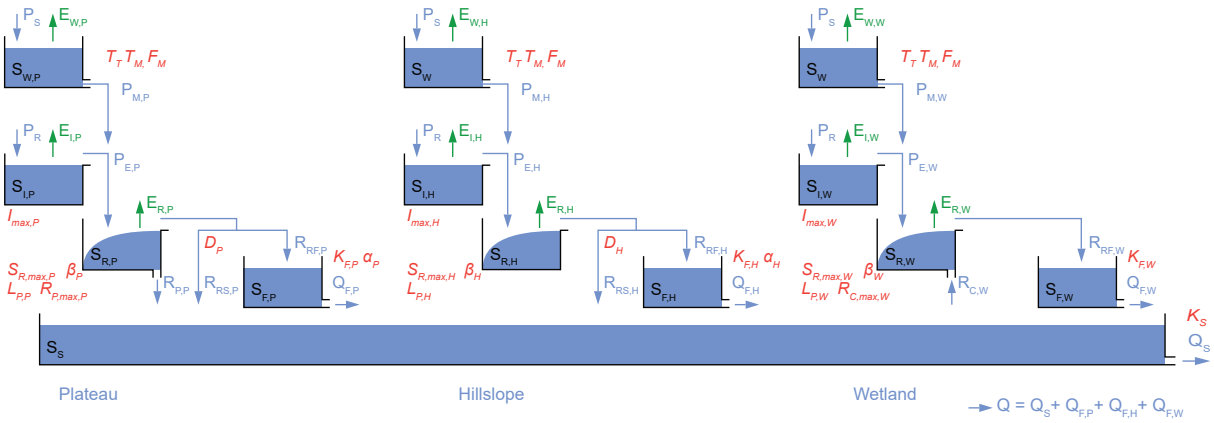

Figure S2: Schematic representation of the wflow_FLEX-Topo model with three HRUs for plateau, hillslope and wetland connected through their groundwater storage. All symbols are defined in Tables S2, S3 and S6. The subscripts P, H and W are used to distinguish between the three HRUs.

Table S2: Definitions of the symbols used to denote the different model fluxes. For each class, the subscripts P, H and W are added in Fig. S2 to denote plateau, hillslope and wetland, e.g. $E_{\mathrm{I,W}}$ indicates interception evaporation from the wetland class.

Fluxes (mm d^{-1})	Definition
P	Precipitation
P_{R}	Rainfall
P_{S}	Snowfall
P_{M}	Snow melt
E_{P}	Potential evaporation
E_{W}	Evaporation from snow storage
E_{I}	Evaporation from interception
E_{R}	Evaporation from the root-zone storage
P_{E}	Effective precipitation
R_{R}	Outflow from the root-zone storage
R_{RS}	Recharge to the slow storage
R_{RF}	Recharge to the fast storage
R_{P}	Percolation
R_{C}	Capillary rise
Q_{F}	Fast runoff
Q_{S}	Slow runoff
Q	Streamflow

Table S3: Definitions of the symbols used to denote the different storages.

Storage (mm)	Definition
S_{W}	Snow storage
S_{I}	Interception storage
S_{R}	Root-zone storage
S_{F}	Fast runoff storage
S_{S}	Slow runoff storage

Table S4: Water balance equations for each class of the wflow_FLEX-Topo model. The three classes share a common groundwater storage S_{S}.

Water balance equation	Plateau	Hillslope	Wetland
$\mathrm{d}S_{\mathrm{W}}/\mathrm{d}t = P_{\mathrm{S}} - E_{\mathrm{W}} - P_{\mathrm{M}}$	✓	✓	✓
$\mathrm{d}S_{\mathrm{I}}/\mathrm{d}t = P_{\mathrm{R}} - E_{\mathrm{I}} - P_{\mathrm{E}}$	✓	✓	✓
$\mathrm{d}S_{\mathrm{R}}/\mathrm{d}t = P_{\mathrm{E}} + P_{\mathrm{M}} - E_{\mathrm{R}} - R_{\mathrm{RS}} - R_{\mathrm{RF}} - R_{\mathrm{P}}$	✓		
$\mathrm{d}S_{\mathrm{R}}/\mathrm{d}t = P_{\mathrm{E}} + P_{\mathrm{M}} - E_{\mathrm{R}} - R_{\mathrm{RS}} - R_{\mathrm{RF}}$		✓	
$\mathrm{d}S_{\mathrm{R}}/\mathrm{d}t = P_{\mathrm{E}} + P_{\mathrm{M}} - E_{\mathrm{R}} - R_{\mathrm{RS}} - R_{\mathrm{RF}} + R_{\mathrm{C}}$			✓
$\mathrm{d}S_{\mathrm{F}}/\mathrm{d}t = R_{\mathrm{RF}} - Q_{\mathrm{F}}$	✓	✓	✓
$\mathrm{d}S_{\mathrm{S}}/\mathrm{d}t = R_{\mathrm{RS}} + R_{\mathrm{P}} - Q_{\mathrm{S}}$	✓		
$\mathrm{d}S_{\mathrm{S}}/\mathrm{d}t = R_{\mathrm{RS}} - Q_{\mathrm{S}}$		✓	
$\mathrm{d}S_{\mathrm{S}}/\mathrm{d}t = -R_{\mathrm{C}} - Q_{\mathrm{S}}$			✓
$Q = Q_{\mathrm{S}} + Q_{\mathrm{F,P}} + Q_{\mathrm{F,H}} + Q_{\mathrm{F,W}}$			

Table S5: Constitutive functions. T denotes temperature. The groundwater storage is shared between all classes. Symbols for the parameters are detailed in Table S6.

Constitutive functions	Plateau	Hillslope	Wetland
Snow			
$P_{\mathrm{S}} = \begin{cases} \mathsf{P}, & \text{if } T < T_{\mathrm{T}} \\ 0, & \text{if } T \geq T_{\mathrm{T}} \end{cases}$	✓	✓	✓
$E_{\mathrm{W}} = \min(E_{\mathrm{P}}, S_{\mathrm{W}}/\mathsf{dt})$	✓	✓	✓
$P_{\mathrm{M}} = \begin{cases} 0, & \text{if } T < T_{\mathrm{T}} \\ \min(\mathsf{F}_{\mathrm{M}} \cdot (T - T_{\mathrm{M}}), S_{\mathrm{W}}/\mathrm{d}t), & \text{if } T \geq T_{\mathrm{T}} \end{cases}$	✓	✓	✓
Interception			
$\overline{S_{\mathrm{I}}} = S_{\mathrm{I}}/I_{\max}$	✓	✓	✓
$P_{\mathrm{R}} = \begin{cases} 0, & \text{if } T < T_{\mathrm{T}} \\ \mathsf{P}, & \text{if } T \geq T_{\mathrm{T}} \end{cases}$	✓	✓	✓
$P_{\mathrm{E}} = \max(0, (S_{\mathrm{I}} - I_{\max})/\mathrm{d}t)$	✓	✓	✓
$E_{\mathrm{I}} = \min(E_{\mathrm{P}} - E_{\mathrm{W}}, S_{\mathrm{I}}/\mathrm{d}t)$	✓	✓	✓
Root-zone			
$\overline{S_{\mathrm{R}}} = S_{\mathrm{R}}/S_{\mathrm{R,max}}$	✓	✓	✓
$R_{\mathrm{R}} = R_{\mathrm{RS}} + R_{\mathrm{RF}}$	✓	✓	
$E_{\mathrm{R}} = \min((E_{\mathrm{P}} - E_{\mathrm{I}}) \cdot \min(\overline{S_{\mathrm{R}}}/L_{\mathrm{P}}, 1), S_{\mathrm{R}}/\mathrm{d}t)$	✓	✓	✓
$R_{\mathrm{R}} = (P_{\mathrm{E}} + P_{\mathrm{M}}) \cdot (1 - (1 - \overline{S_{\mathrm{R}}})^{\beta})$	✓	✓	✓
$R_{\mathrm{P}} = R_{\mathrm{P,max}} \cdot \overline{S_{\mathrm{R}}}$	✓		
$R_{\mathrm{C}} = R_{\mathrm{C,max}} \cdot (1 - \overline{S_{\mathrm{R}}})$			✓
Fast storage			
$R_{\mathrm{RF}} = R_{\mathrm{R}} \cdot (1 - D)$	✓	✓	
$R_{\mathrm{RF}} = R_{\mathrm{R}}$			✓
$Q_{\mathrm{F}} = K_{\mathrm{F}}^{-1} \cdot S_{\mathrm{F}}^{\alpha}$	✓	✓	
$Q_{\mathrm{F}} = K_{\mathrm{F}}^{-1} \cdot S_{\mathrm{F}}$			✓
Slow storage			
$R_{\mathrm{RS}} = R_{\mathrm{R}} \cdot D$	✓	✓	
$Q_{\mathrm{S}} = K_{\mathrm{S}}^{-1} \cdot S_{\mathrm{S}}$	✓	✓	✓

S4 Prior and posterior parameter distributions

A description of model parameters, units, prior and posterior ranges is provided in Table S6. To deal with the relatively long computational costs of running the model, we applied a preliminary first calibration to pre-scan the range of prior distributions. The real calibration was performed with these reduced parameter ranges as prior, which explains the limited difference between prior and posterior distributions. We retained 124 parameter sets based on the defined criteria for model performance.

Table S6: Calibrated model parameters, units and prior range (*MRC denotes the value determined with a master recession curve ± 30 %).

Parameter	unit	Description	Prior range	Posterior Plateau	Posterior Hillslope	Posterior Wetland
T_{T}	°C	Threshold temp. snow and rain	0.7 - 1.9	0.7 - 1.7	0.7 - 1.7	0.7 - 1.7
T_{M}	°C	Threshold temp. snow melt	0.7 - 2.3	0.8 - 2.2	0.8 - 2.2	0.8 - 2.2
F_{M}	mm d^{-1} $^{\circ}\mathrm{C}^{-1}$	Degree day factor	2.0 - 5.0	2.3 - 5.0	2.3 - 5.0	2.3 - 5.0
$I_{\max}$	mm	Max. interception capacity	0.5 - 4.0	0.5 - 3.0	0.9 - 4.0	0.5 - 3.0
β	-	Shape parameter	0.2 - 0.4	0.2 - 0.4	0.2 - 0.4	0.2 - 0.4
L_{P}	-	Evap. reduction coefficient	0.1 - 0.6	0.1 - 0.6	0.1 - 0.4	0.1 - 0.6
$R_{\mathrm{C,max,W}}$	mm d^{-1}	Max. capillary rise	0.1 - 0.5			0.1 - 0.5
$R_{\mathrm{P,max,P}}$	mm d^{-1}	Max. percolation	0.05 - 0.72	0.05 - 0.72		
α	-	Non-linear coefficient	1 - 1.8	1.0 - 1.8	1.0 - 1.4	
K_{F}	d	Fast recession time scale	10 - 100	10 - 100	10 - 100	10 - 100
D	-	Fraction to slow storage	0.04 - 1	0.05 - 1	0.05 - 1	
K_{S}	d	Slow recession time scale	MRC*			

S5 Hydrological model results with the simulated historical climate data and root-zone storage capacity derived from this data

In the manuscript, the observed historical E-OBS climate data is used to calibrate the model and to estimate the root-zone storage capacity parameter $S_{\mathrm{R,max,A}}$ for the historical climate and land-use conditions, as it is assumed to best represent current-day conditions. The parameter $S_{\mathrm{R,max,A}}$ is subsequently used for the model run forced with the simulated historical climate data. For the model runs with the simulated 2K climate data, we adapt the historical root-zone storage capacity $S_{\mathrm{R,max,A}}$ by adding the increase in storage deficit between the simulated historical and 2K climate data to the observed historical storage deficit to obtain $S_{\mathrm{R,max,B}}$ (Table S1).

Another approach would have been to estimate an alternative root-zone storage capacity parameter $S_{\mathrm{R,max,A1}}$ for the historical period, using the simulated historical climate data instead of the observed historical E-OBS climate data (Table S1). This has the advantage that potential biases in the simulated historical climate data are directly corrected for in the estimation of the root-zone storage capacity parameter. However, these biases may also result in a less plausible spatial representation of the root-zone storage capacity across catchments of the Meuse basin.

In the estimation of the root-zone storage capacity $S_{\mathrm{R,max,A1}}$ using the simulated historical climate data, the long term transpiration is calculated according to $E_{\mathrm{R}} = P_{\mathrm{E,hist}} - Q_{\mathrm{obs}}/P_{\mathrm{hist}} \cdot P_{\mathrm{hist}}$, with the subscript $_{\mathrm{hist}}$ to denote the simulated historical climate data (Table S1). The resulting root-zone storage capacity values are slightly higher than $S_{\mathrm{R,max,A}}$ with 110 $\pm$ 18 mm and 179 $\pm$ 28 mm for 2 and 20 years return periods, respectively. This corresponds to an overestimation of about +7 % in comparison to $S_{\mathrm{R,max,A}}$, which is due to the higher precipitation (on average +9 %, Fig. S3) in the simulated historical climate data compared to the observed E-OBS historical data, which leads to relatively lower runoff coefficients and therefore larger evaporative indices and storage deficits in the water balance calculation of the root-zone storage capacity.

The model run forced with the simulated historical climate data and the larger root-zone storage capacity $S_{\mathrm{R,max,A1}}$ results in slightly lower peak flows and mean monthly winter streamflow in comparison to the model run with the simulated historical climate data and the $S_{\mathrm{R,max,A}}$ parameter (Fig. S4). However, differences are relatively small and the hydrological behavior of the three historical runs (E-OBS with $S_{\mathrm{R,max,A}}$, simulated historical with $S_{\mathrm{R,max,A}}$ and simulated historical with $S_{\mathrm{R,max,A1}}$) is relatively similar (Fig. S4). The model runs forced with the simulated historical climate data and with both $S_{\mathrm{R,max,A}}$ and $S_{\mathrm{R,max,A1}}$ as model parameter also show similar performance metrics (Fig. S5).

These analyses suggest that hydrological model performance for the historical period is slightly improved if the root-zone storage capacity parameter is adapted to the used forcing data. However, these improvements between using $S_{\mathrm{R,max,A}}$ and $S_{\mathrm{R,max,A1}}$ in model runs forced with the simulated historical climate data are relatively small.

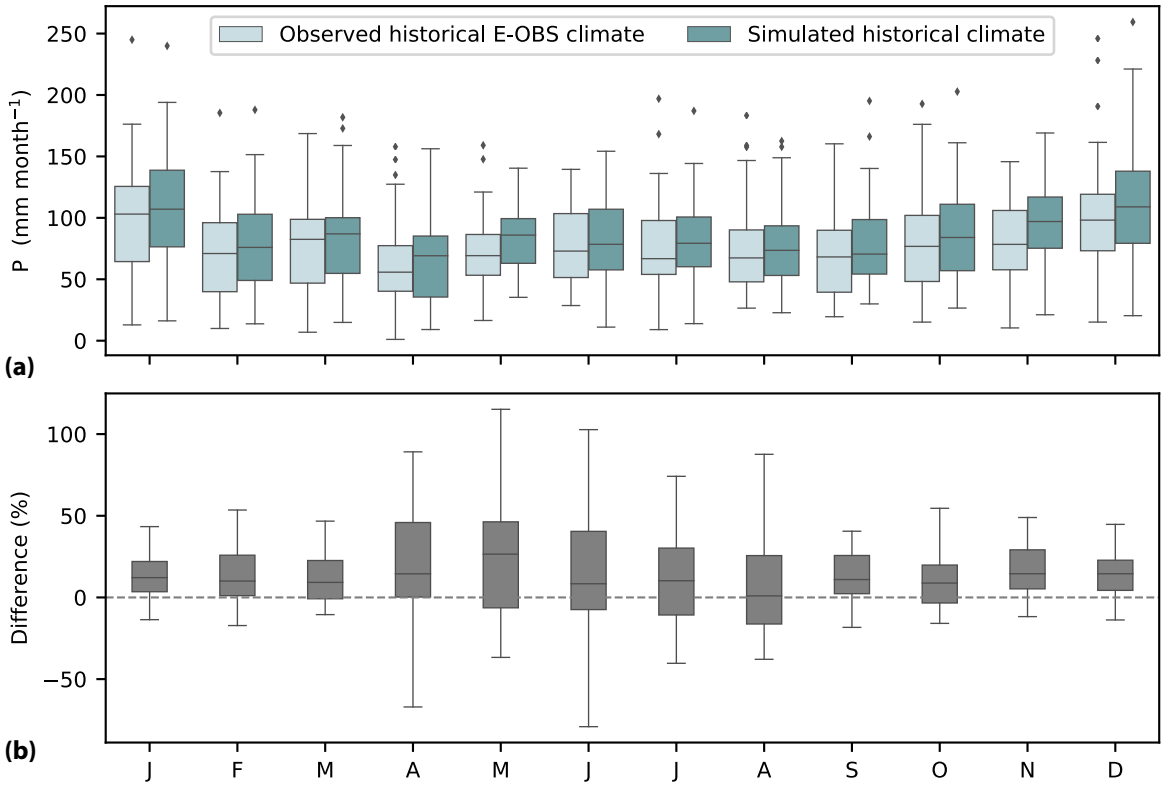

Figure S3: **(a)** Mean monthly precipitation of the observed E-OBS and simulated historical climate data for the period 1980-2018 and **(b)** difference between the simulated and observed monthly precipitation (%).

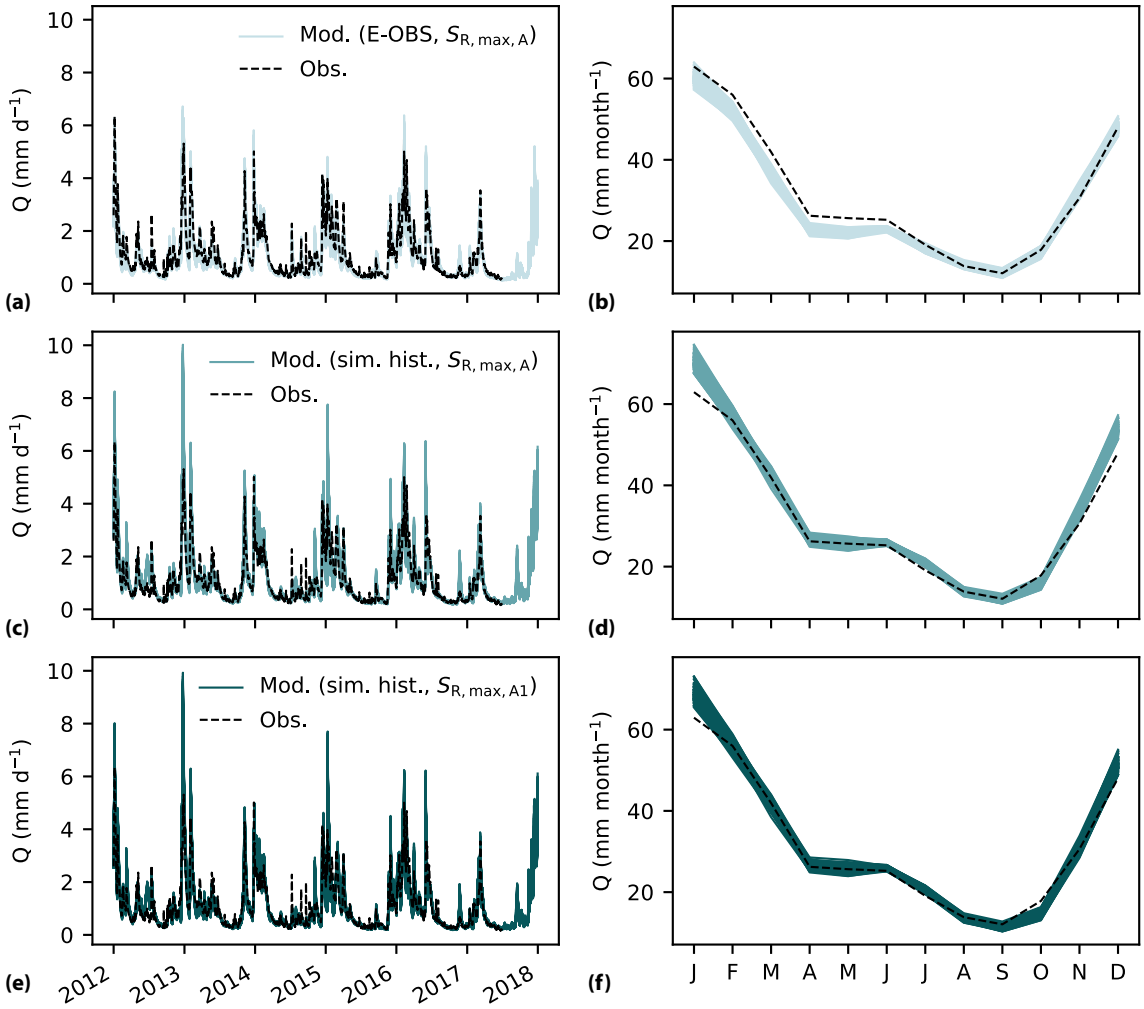

Figure S4: Observed and modeled hydrographs and mean monthly streamflow at Borgharen for the ensemble of parameter sets retained as feasible after calibration when the model is: **(a,b)** forced with E-OBS historical data and using $S_{\mathrm{R,max,A}}$ as model parameter, **(c,d)** forced with the simulated historical climate data using $S_{\mathrm{R,max,A}}$ as model parameter, and **(e,f)** forced with the simulated historical climate data using $S_{\mathrm{R,max,A1}}$ as model parameter. The panels **(a,b,c,d)** are repeated from the manuscript to allow for a better comparison with the added panels **(e,f)**.

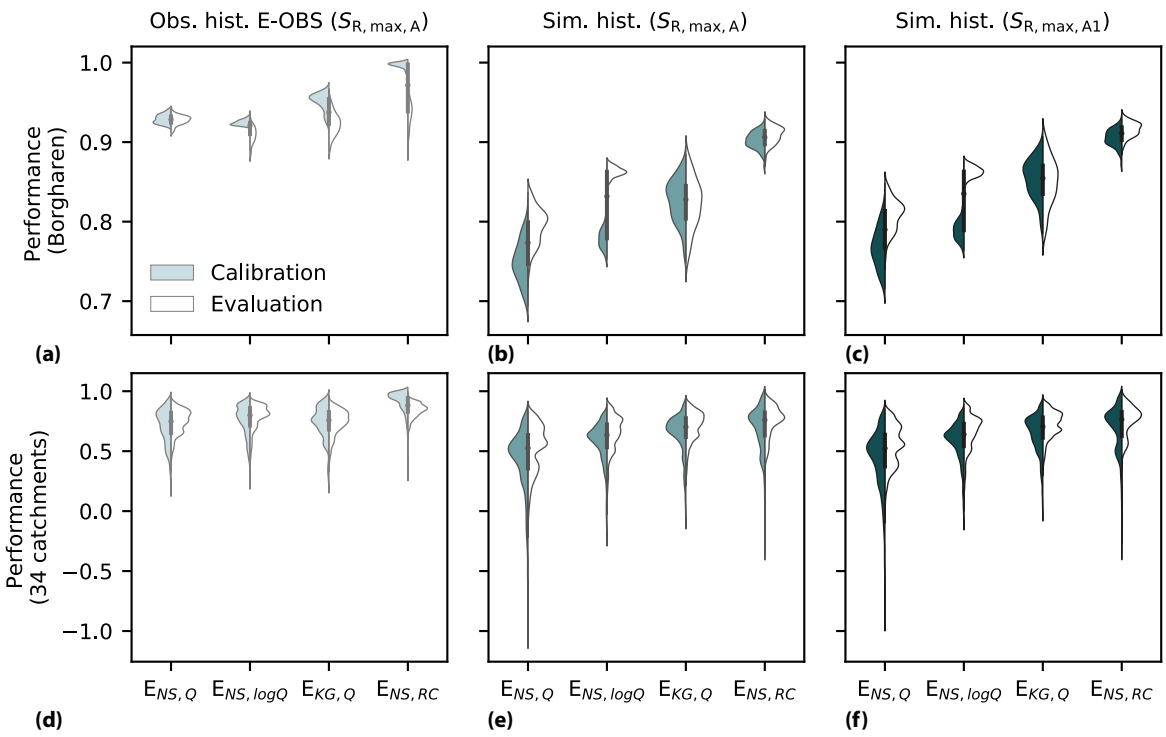

Figure S5: Streamflow model performance during calibration and evaluation for the four objective functions when the model is forced with (**a,d**) observed historical E-OBS data and $S_{\mathrm{R,max,A}}$ as model parameter, (**b,e**) simulated historical climate data and $S_{\mathrm{R,max,A}}$ as model parameter, and (**c,f**) simulated historical climate data and $S_{\mathrm{R,max,A1}}$ as model parameter at (**a,b,c**) Borgharen and (**d,e,f**) for the ensemble of nested catchments in the Meuse basin. The four objective functions are the Nash-Sutcliffe efficiencies of streamflow, logarithm of streamflow and monthly runoff coefficient ($E_{\mathrm{NS,Q}}$, $E_{\mathrm{NS,logQ}}$, $E_{\mathrm{NS,RC}}$) as well as the Kling-Gupta efficiency of streamflow ($E_{\mathrm{KG,Q}}$). Note the different y-axis between rows. The panels **(a,b,d,e)** are repeated from the manuscript to allow for a better comparison with the added panels **(c,f)**.

References

Bouaziz, L. J. E., Steele-Dunne, S. C., Schellekens, J., Weerts, A. H., Stam, J., Sprokkereef, E., Winsemius, H.C., Savenije, H.H.G & Hrachowitz, M.: Improved understanding of the link between catchment-scale vegetation accessible storage and satellite-derived Soil Water Index, Water Resources Research, 56(3), e2019WR026365, https://doi.org/10.1029/2019WR026365, 2020.

Ehret, U., Zehe, E.,Wulfmeyer, V.,Warrach-Sagi, K., and Liebert, J.: HESS Opinions "should we apply bias correction to global and regional climate model data?", Hydrology and Earth System Sciences, 16, 3391–3404, https://doi.org/10.5194/hess-16-3391-2012, 2012.